Trade-offs of lipid remodelling in a marine predator-prey interaction in response to phosphorus limitation

Richard Guillonneau[1], Andrew R. J. Murphy[1], Zhao-Jie Teng[2,3], Peng Wang[2], Yu-Zhong Zhang[2,3], David J Scanlan[1], Yin Chen[1]

[1] School of Life Sciences, University of Warwick, Coventry, CV4 7AL, United Kingdom

[2] College of Marine Life Sciences, and Frontiers Science Center for Deep Ocean Multispheres and Earth System, Ocean University of China, Qingdao, China.

[3] State Key Laboratory of Microbial Technology, Marine Biotechnology Research Center, Shandong University, Qingdao, China.

Correspondence to Dr R Guillonneau (richard.guillonneau@warwick.ac.uk) or Prof. Y Chen (y.chen.25@warwick.ac.uk)

Classification: Biological Sciences/ Environmental Sciences and Ecology

Keywords: predation, marine ciliate, roseobacters, lipid remodelling, phosphorus limitation

Abstract:

Phosphorus (P) is a key nutrient limiting bacterial growth and primary production in the oceans. Unsurprisingly, marine microbes have evolved sophisticated strategies to adapt to P limitation, one of which involves the remodelling of membrane lipids by replacing phospholipids with non-P containing surrogate lipids. This strategy is adopted by both cosmopolitan marine phytoplankton and heterotrophic bacteria and serves to reduce the cellular P quota. However, little if anything is known of the biological consequences of lipid remodelling. Here, using the marine bacterium *Phaeobacter* sp. MED193 and the ciliate *Uronema marinum* as a model, we sought to assess the effect of remodelling on bacteria-protist interactions. We discovered an important trade-off between either escape from ingestion or resistance to digestion. Thus, *Phaeobacter* grown under P-replete conditions was readily ingested by *Uronema* but not easily digested, supporting only limited predator growth. In contrast, following membrane lipid remodelling in response to P-depletion, *Phaeobacter* was less likely to be captured by *Uronema* thanks to the reduced expression of mannosylated glycoconjugates. However, once ingested, membrane remodelled cells were unable to prevent phagosome acidification, became more susceptible to digestion and, as such, allowed rapid growth of the ciliate predator. This trade-off between adapting to a P-limited environment and susceptibility to protist grazing suggests the more efficient removal of low P prey that potentially has important implications for the functioning of the marine microbial food web in terms of trophic energy transfer and nutrient export efficiency.

Significance statement

Microbial growth is often limited by key nutrients like phosphorus (P) across the global ocean. A major response to P limitation is the replacement of membrane phospholipids with non-P lipids to reduce their cellular P quota. However, the biological 'costs' of lipid remodelling are largely unknown. Here, we uncover a predator-prey interaction trade-off whereby a lipid remodelled bacterial prey cell becomes more susceptible to digestion by a protozoan predator facilitating its rapid growth. Thus, we highlight a complex interplay between adaptation to the abiotic environment and consequences for biotic interactions (grazing), which may have important implications for the stability and structuring of microbial communities and the performance of the marine food web.

Introduction

Bacteria play fundamental roles in the functioning of the ocean ecosystem being at the base of marine food webs and via mediating key biogeochemical cycles (1-3). One of the key nutrients that constrains microbial growth in the oceans is phosphorus (P) (4), with e.g. the North Atlantic Ocean and the Mediterranean Sea being well known P-limited environments (5-8). P is an essential element for all cells, forming the backbone of nucleic acids, ATP and membrane phospholipids. P limitation can also affect the complex interplay between heterotrophic bacteria and phytoplankton, thus influencing trophic interactions and the cycling of organic matter (9, 10). Global change is expected to exacerbate P limitation in the surface ocean due to water column stratification accelerated by global warming (11). As such, it is not surprising that marine microbes have evolved sophisticated mechanisms to cope with P limitation with one such strategy being the substitution of membrane phospholipids by non-P containing surrogate lipids. Indeed, during P deficiency, both photosynthetic cyanobacteria and algae (12) as well as heterotrophic bacteria of the SAR11 and roseobacter clades are capable of reducing their consumption of P by substituting membrane phospholipids with non-P containing versions (13-15). In heterotrophic bacteria, this so-called lipid remodelling pathway is mediated by the *plcP* encoded phospholipase C enzyme (16, 17). Previous metagenomics analysis estimates that up to one quarter of bacteria in surface ocean assemblages possess the *plcP* gene (14, 18). Indeed, its abundance appears to be a reliable biomarker for phosphate availability in marine surface waters (6). We and others have also shown that PlcP-mediated lipid remodelling occurs naturally in surface seawater microbial assemblages (see (14, 18). Thus, non-P lipids, primarily glycolipids and betaine lipids, have been shown to account for >70% of the polar lipids in summer when P is severely limited but only ~ 30% in the autumn when P-limitation is alleviated (14).

It has become increasingly evident that the ability to perform lipid remodelling offers a competitive advantage to bacteria saving up to 50-86% of cellular P demand (13, 14), although genome streamlining may also play a role in this respect (19, 20). However, it remains unknown whether such a drastic change in membrane composition has unforeseen consequences for other

77 aspects of bacterial physiology, particularly how these organisms interact with their biotic
78 environment. In general terms the abundance of marine microbes is governed by the interplay
79 between abiotic (light, nutrients including P) and biotic (viral lysis and protist grazing) factors (21),
80 which dictates the overall balance between bacterial growth and mortality, and ultimately their
81 population size in the global ocean. Whilst much is known of the consequences of biotic controls on
82 the mortality of marine microbes (22, 23), with estimates suggesting that almost all the daily bacterial
83 production can be removed by viral lysis and protozoan grazing (21, 24), much less is known about
84 how these biological controls are affected by the abiotic environment. This is especially the case when
85 considering the interplay between cosmopolitan marine bacteria and protist predators and,
86 particularly, how adaptation to the abiotic nutrient environment affects predator-prey interactions
87 (25, 26). Protists are one of the most diverse and abundant groups of marine microbes (27-29),
88 amongst which the ciliates are an important taxon with a global distribution (30) capable of exerting
89 considerable selective pressure on bacterioplankton dynamics through grazing. Indeed, ciliates can
90 directly influence the structure and abundance of dominant marine heterotrophic bacteria such as
91 the marine roseobacter clade that are key players in key biogeochemical cycles via their formation of
92 climate-active trace gases such as dimethylsulfide and methylamines (31, 32).

93 Here, we specifically set out to investigate the interplay between abiotic and biotic factors in
94 controlling interactions between marine microbes. Using a marine ciliate, *Uronema marinum*, and a
95 marine roseobacter clade bacterium (*Phaeobacter* sp. MED193) as a model, we examine how the
96 dynamics of prey-predator interactions are influenced by P availability. We reveal an important trade-
97 off for a lipid remodelled prey which is more susceptible to digestion by a ciliate predator compared
98 to its unmodelled counterpart despite the latter being more readily ingested by the predator.

Results

Establishing a model system to investigate the impact of predator-prey interactions under phosphorus limitation

We first examined the active prevalence of PlcP mediated lipid remodelling across the global ocean using Tara Oceans metatranscriptome datasets. In agreement with previous analyses of metagenomics datasets, which showed the high abundance of the *plcP* gene in the North Atlantic Ocean, Red Sea and Mediterranean Sea (**Fig. 1A**) (6, 13, 14), on average ~20% of surface marine bacteria have *plcP*. In the Mediterranean Sea, transcription of *plcP* was >10-fold higher (**Fig. 1B**) than other ocean regions that are not typically P-limited such as the Southern Ocean (4), highlighting the importance of lipid remodelling as a key process enabling the proliferation of marine microbes inhabiting P-deplete oceanic waters. Given the high expression of *plcP* in the Mediterranean Sea, Red Sea and North Atlantic Ocean, we used a model marine roseobacter clade bacterium, *Phaeobacter* sp. MED193, originally isolated from these Mediterranean waters (33) as prey, and which is already known to undergo lipid remodelling during P-deplete growth (12). Similarly, as a model predator, we used the marine ciliate *Uronema marinum* (hereafter *Uronema*) which has been readily isolated from the Mediterranean Sea (34, 35) but is globally distributed (**Fig. 1C**) being widely reported in numerous studies (**Supp. Table 1**).

Lipid remodelled *Phaeobacter* sp. MED193 prey is less readily ingested by the ciliate predator

Because the bacterial cell membrane is one of the first points of contact during predation by phagotrophic cells, we first examined predator-prey interactions during short-term feeding experiments (**Fig. 2**). Confocal microscopy showed that when *Uronema* fed on wild-type (WT) *Phaeobacter* prey labelled with GFP to aid visualisation within the ciliate and cultivated in P-replete artificial seawater (ASW), a higher number of prey was observed inside the predator than the same prey cultured under P-deplete conditions (**Fig. 2A**). This suggested that lipid remodelled prey were less likely to be captured by the predator and that substitution of membrane phospholipids by non-P

containing lipids (i.e. diacylglyceryltrimethylhomoserine - DGTS in *Phaeobacter* sp. MED193) facilitated prey escape from predation. Given that a *Phaeobacter* sp. MED193 Δ*plcP* mutant is unable to perform lipid remodelling and hence cannot produce the surrogate lipid DGTS (14), we investigated whether predator-prey interactions were affected in the Δ*plcP* mutant. We found no difference in ingestion of the Δ*plcP* mutant prey, i.e. no obvious differences in prey numbers inside the protist, regardless of whether the mutant prey was cultured in P-replete or P-deplete conditions (**Fig. 2B**). Lipidomics analysis confirmed that lipid remodelling (evidenced by formation of DGTS) only occurred in WT prey cultivated under P-deplete conditions whilst the Δ*plcP* mutant did not produce DGTS under either P-deplete or P-replete growth conditions (**Fig. 2C**, **Suppl. Fig. S1**). Together, these results suggest that the ciliate is capable of differentiating prey types depending on their ability to perform lipid remodelling and synthesis of non-P surrogate membrane lipids.

To more quantitatively assess this difference in prey preference we analysed the ingestion rate, i.e. the number of bacteria ingested per min, using either WT or Δ*plcP* mutant prey. When consuming WT GFP-labelled prey cultivated under P replete conditions, *Uronema* was able to ingest 2.55 ± 1.45 bacteria/min whilst for the same prey grown under P deplete conditions *Uronema* only ingested 1.51 ± 0.66 bacteria/min (**Fig. 2D**). In contrast, there was no difference in ingestion rate with Δ*plcP* mutant prey grown under P replete and P deplete conditions (**Fig. 2D**). We also analysed the percentage of protozoa containing prey using WT or Δ*plcP* mutant (**Fig. 2E**). Thus, after 5 min of interaction, 84 ± 0.2 % of protozoa contained prey when interacted with WT grown under P-replete conditions, but the number reduced to 58 ± 1.5 % when WT prey was cultivated under P-deplete conditions. Conversely, no difference in the percentage of protozoa containing prey was observed when the Δ*plcP* mutant was grown under P-replete/-deplete conditions (**Fig. 2E**). Together, these results support the notion that P stress induced membrane lipid remodelling facilitates prey escape from ciliate predation.

Escape from ciliate ingestion involves mannosylated glycoconjugates but not size selection

We then set out to investigate the underlying mechanism for the apparent predator avoidance of lipid remodelled prey. Since protists are well known for selecting prey according to size (36), we first examined whether there was a difference in size between the WT and Δ*plcP* mutant grown under P replete and P deplete conditions. However, no obvious size differences were observed (**Fig. 2F**). In addition to size, masking the cell surface is another common strategy adopted by prey to avoid ingestion by protists (36). We therefore investigated whether the formation of surrogate membrane lipids under P deplete conditions affected prey capture by predator phagocytic receptors, among which the mannose receptor is strikingly conserved across the eukaryotic domain (37) and known to be used as a feeding receptor for recognising prey (38). We studied whether there was a noticeable difference in mannose-decorated glycoconjugates in WT and *plcP* mutant prey grown under P-replete and P-deplete conditions using a mannose-binding lectin (Concanavalin A) labelled with rhodamine. When WT prey was grown in P-replete medium substantially more rhodamine-labelling was detected by confocal microscopy (**Fig. 2G, 2H**) compared to the same prey grown under P-deplete conditions where the rhodamine signal was significantly reduced (**Fig. 2G, 2H**). This difference in rhodamine labelling was not observed with Δ*plcP* mutant prey which is unable to perform lipid remodelling (**Fig. 2G, 2H**). These results suggest that the formation of surrogate lipids in response to P limitation reduces the level of mannose-containing glycoconjugates on the prey cell surface.

To further support the involvement of mannose receptors in prey capture by *Uronema* a short-term ingestion experiment was performed using ciliates that had been pre-incubated with mannosylated bovine serum albumin (BSA-mannose) as a decoy. After incubation of the predator with BSA-mannose, a significantly lower rate of bacteria was ingested by the protozoa, corresponding to 0.89 ± 0.71 bacteria/min and 0.45 ± 0.57 bacteria/min for the WT grown under P replete or P deplete medium, respectively (**Fig. 2D**). Together, these experiments suggest lipid remodelling in response to P limitation affects mannosylated macromolecules that are involved in prey-predator recognition.

The ciliate predator is capable of selective grazing with a preference for prey incapable of lipid remodelling

Since prey carrying out lipid remodelling reduce the expression of mannose-containing glycoconjugates, which in turn reduces ingestion by the predator, we hypothesized this would result in selective grazing by the predator in a mixed prey community. To test this idea, we carried out three types of predation experiments using 1) WT prey grown under P-replete conditions mixed with WT prey grown under P-deplete conditions; 2) WT prey and Δ*plcP* mutant prey both cultivated under P-replete conditions and 3) WT prey and Δ*plcP* mutant prey both cultivated under P-deplete conditions. To facilitate microscopy of the prey inside the ciliate, WT and Δ*plcP* mutant prey were labelled with GFP and mCherry depending on the growth condition, for subsequent confocal imaging.

When the ciliate had the choice to feed on WT prey that was previously cultivated in a medium either replete or deplete in P (the latter condition causing lipid remodelling), the ciliate preferentially ingested prey that had not undergone lipid remodelling. Thus, after 5 min of interaction there were 60.3 ± 5.4% P-replete prey but only 39.7 ± 5.4% P-deplete prey (**Fig. 3A, Fig. 3B top panel**). In contrast, when the ciliate had the choice between WT and Δ*plcP* mutant prey that had both been grown under P-replete conditions *Uronema* showed no significant prey preference ($P>0.05$ **Fig. 3A, Fig. 3B middle panel)** consistent with no lipid remodelling occurring under these conditions. Finally, *Uronema* given the choice of WT and Δ*plcP* mutant prey both grown in P-deplete medium (and hence with only WT prey having undergone lipid remodelling), the ciliate displayed a clear preference for the Δ*plcP* mutant ($P<0.05$) **Fig. 3A, Fig. 3B lower panel**). Together, these selective grazing experiments using a mixed prey community support the finding that a lipid remodelled prey has a selective advantage over its non-modelled counterpart by reducing its susceptibility to protist ingestion.

A lipid remodelled prey supports better growth of the ciliate

Having established that lipid remodelling facilitates the escape of prey from ingestion by the ciliate predator, we next examined the fate of prey in a long-term interaction experiment performed up to

72 hours. Interestingly, WT prey capable of lipid remodelling supported better growth of the ciliate at all three multiplicity-of-infections (MOIs) tested (**Fig. 4A**). Thus, after 24h of interaction at a MOI of 500, *Uronema* cell densities reached 53,480 ± 5,517 cells/mL when fed on P-deplete prey compared to 34,370 cells/mL when fed on P-replete prey (**Fig. 4A**). Concomitantly, a sharp decrease in prey numbers occurred between 3h and 24h of interaction (**Fig. 4B**). The same trends were seen with MOIs of 100 and 10. Growth of the predator at 24h interaction was much reduced when consuming P-deplete Δ*plcP* mutant prey (ca 18,889 ± 8,694 cells/ml) that is unable to perform lipid remodelling (**Fig. 4C**) and there was little difference in *Uronema* growth when fed on P-replete/-deplete Δ*plcP* mutant grown prey. Consequently, Δ*plcP* mutant prey abundance decreased only slightly across the experiment (**Fig. 4D**). Control experiments demonstrated that medium alone did not support *Uronema* or *Phaeobacter* growth and that the addition of Triton-X100 to release bacteria from protozoa had no impact on prey viability (**Supp. Fig. S2**). This significantly better *Uronema* growth when fed WT prey that has undergone lipid remodelling (**Fig. 4A**) suggests that lipid remodelled prey cells are more easily digested by the ciliate once ingested.

Lipid remodelled prey is more susceptible to digestion

In order to understand the fate of lipid remodelled prey inside the ciliate, co-localization studies were performed by tracking phagolysosome acidification after prey engulfment using the LysoTracker™ Red DND-99 stain which specifically stains acidic organelles in live cells. Confocal imaging showed intensive acidification of prey-containing vacuoles after 3 h interaction between *Uronema* and WT prey grown under P-deplete conditions, whereas WT prey cultivated under P-replete conditions markedly reduced acidification of the vacuoles (**Fig. 5A**). The Δ*plcP* mutant was also capable of largely preventing vacuole acidification regardless of whether it was cultivated in P-replete or P-deplete conditions. Thus, a quantitative analysis showed that only 39.4 ± 6.7% of bacteria-containing vacuoles were acidified when *Uronema* was fed P-replete prey compared to 73.8 ± 5.5% bacteria-containing vacuoles being acidified when fed P-deplete WT prey (**Fig. 5B**). Corresponding data for Δ*plcP* mutant prey grown

under P-replete/P-deplete conditions was 26.8 ± 5.1% and 31.0 ± 2.1%, respectively. Taken together, these results suggest that, once ingested, lipid remodelled prey is unable to prevent acidification of the phagosome and, as such, is better digested by the ciliate, therefore supporting higher *Uronema* cell abundances.

Such an idea is further supported by analysis of food-containing vacuoles in mixed predator-prey interaction experiments. After 3h, 10 h and 24 h interaction between *Uronema* and *Phaeobacter*, when *Uronema* was fed WT and Δ*plcP* mutant prey grown under P-replete conditions, there was no major change in the percentages of the two prey types inside the predator (**Fig. 5D**). However, when WT lipid remodelled prey was mixed with either WT or Δ*plcP* mutant unmodelled prey, the former is selectively digested (**Fig. 5C, 5E**). Together, these data suggest that prey that has undergone lipid remodelling is less able to inhibit phagolysosomal acidification after engulfment, and as such is more easily digested supporting better growth of the predator. Indeed, assessment of *Phaeobacter* survival in medium mimicking acidification (pH 6) and oxidative stress (the presence of hydrogen peroxide) conditions inside a phagolysosome showed that the WT lipid remodelled prey survived poorly at lower pH or in the presence of H_2O_2 compared to its unmodelled counterpart (**Suppl. Fig. S3)**.

Discussion:

The low availability of key nutrients like P in marine surface waters represents a grand challenge for microbes, particularly those inhabiting oligotrophic gyres. Although lipid remodelling enables these microbes to survive better these potentially P limited environments, as well as facilitating greater avoidance of ingestion by ciliate grazers, once ingested, these lipid remodelled cells are unable to survive phagolysosomal digestion (**Fig. 6**). Therefore, these microbes face an unsolvable dilemma. On the one hand, lipid remodelling helps prey escape ingestion by the ciliate, but on the other, prey is more susceptible to insult from the harmful acid and oxidative stress conditions resulting from lysosome fusion and phagosome acidification. We should add though that such a dilemma (between escape from ingestion and resistance to digestion) is not the only trade-off microbes face due to grazing pressure. For example, it is well known that bacteria can form biofilms or clumping (39, 40) to avoid capture by protists at the expense of growth, such morphological changes affecting cell surface area-to-volume ratios which negatively impact on nutrient uptake for optimum growth. Similarly, unicellular algae with larger cell sizes are poorly grazed but have low ammonium uptake rates and grow poorly (41). Equally, *Pseudomonas aeruginosa* isolated from long-term chronically infected patients are less resistant to protist grazing (42). Thus, it is clear that adaptation to a specific niche can come with consequences to an organisms' viability, although it remains to be seen what other trade-offs in predator-prey interactions exist following adaptation of cosmopolitan marine microbes to P limitation.

To capture prey, phagotrophic cells must recognize certain bacterial structures to avoid self-predation or engulfment of inorganic matter (43). One of the most evolutionally conserved structures involved in prey recognition by phagotrophic cells are mannose-binding lectins (44) which are found not only in mammalian macrophages but also protists such as dinoflagellates and ciliates (37). Interestingly, we observed that lipid remodelling induced by prey P limitation impaired decoration of prey cells by mannose-containing glycoconjugates and subsequent ingestion by the ciliate grazer (**Fig. 2G, 2H**) although the identities of these cell-surface mannosylated glycoconjugates remain to be

established. Such an interplay of abiotic control of prey ingestion may be more common than previously expected. For example, it has been noted that a nitrogen-deficient culture of the microalgae *Isochrysis galbana* was also rich in cell surface mannose (45, 46), whilst phosphate limitation appears to play a role in the digestion of green algae by zooplankton (47). Moreover, members of the highly abundant SAR11 clade have a much less hydrophobic cell surface than other planktonic bacteria facilitating filtration evasion by slipping through the mucous nets of marine tunicates (48). This reiterates the importance and complexity of the prey cell surface in predator-prey interactions.

Surprisingly, enhanced ingestion of prey did not translate into better growth of the ciliate predator. Whilst we would have expected better *Uronema* growth when grazing on WT prey that had previously grown in P-replete medium replete due to its higher nutritional quality (49), we observed the opposite (**Fig. 4**). Thus, 24h post-interaction with WT prey cultivated in P replete medium *Uronema* reached a concentration 35% lower (at a MOI of 500) compared to the same prey cultivated in P-deplete medium. Concomitantly, nearly 99% of the prey cultivated in P replete medium were consumed (**Fig. 4B**). It thus appears that lipid unmodelled prey (*i.e.* WT prey grown in P replete conditions or the Δ*plcP* deletion mutant grown under either P-replete or P-deplete conditions - since this mutant is unable to remodel its lipids) is capable of preventing digestion by inhibiting the acidification of the food-containing vacuole. This conclusion is supported not only by co-localizing fluorescence-labelled prey cells with LysoTracker (**Fig. 5A-B**), but also by the evolution of intracellular survival in mixed prey grazing experiments following the pre-culturing of prey under P-replete or P-deplete growth conditions (**Fig. 5C-E**). Interestingly, *in vitro* experiments mimicking phagolysosome acidification and oxidative stress also demonstrates that lipid remodelled prey are significantly more sensitive to killing by low pH and oxidative stress (**Suppl. Fig. 2**). Although it is unclear how membrane lipid remodelling prevents acidification of the food-containing vacuoles in this ciliate, it is possible that some type of bacterial effector is released by the prey in response to mannose-binding lectin dependent phagocytosis in order to prevent the formation or subsequent acidification of the

295 phagolysosome. In this regard, such a prey-ciliate interaction resembles pathogen clearance by
296 professional human phagocytes such as macrophages (50). Certainly, marine roseobacters are known
297 to produce toxins (51, 52) that are capable of inhibiting the growth of, or even killing, eukaryotic
298 phytoplankton (52-54). Thus the role of lipid remodelling in bacteria-eukaryote interactions clearly
299 warrants further investigation.

300 Overall, our data highlights a new avenue in predator-prey interactions, namely how these
301 interactions can be governed by nutrient availability via the remodelling of membrane lipids that takes
302 place under P-deplete growth conditions (**Fig. 6**). In the model *Phaeobacter* sp. we utilise here,
303 remodelling reduces its P consumption by replacing membrane phospholipids (primarily
304 phosphatidylglycerol and phosphatidylethanolamine) with alternative non-phosphorus lipids (e.g.
305 DGTS) (14). The fact that this lipid remodelling process is occurring naturally in P-deplete oceanic
306 waters across not only heterotrophic bacteria (13, 14) but also cyanobacteria and eukaryotic algae
307 (12, 55) is suggestive of a much wider importance of this phenomenon. Extensive lipid remodelling in
308 the natural environment is reiterated not only by metagenomics and transcriptomics data of the *plcP*
309 gene directly involved in remodelling in heterotrophic bacteria at least (Fig. 1B), but also by direct
310 analysis of membrane lipids in natural microbial communities (12, 14, 55, 56). However, how general
311 across different taxonomic groups of predator and prey these effects are, clearly requires further
312 work. Moreover, given the effects of remodelling on predator-prey interactions we report here are
313 ultimately controlled by *in situ* P concentrations (which controls lipid remodelling) then such
314 interaction effects are also likely to be dynamic in their nature given the often seasonal nature of P
315 limitation e.g. in the Mediterranean Sea PlcP-mediated lipid remodelling occurs across an annual cycle
316 whereby P limitation intensifies during spring and summer but starts to become alleviated from
317 September (14, 57). Nonetheless, this work clearly highlights the complex interplay between the
318 abiotic nutrient environment, microbes and their grazers and how predator-prey dynamics are
319 governed by abiotic control of prey physiology which has important implications for how we model

320 trophic interactions in marine ecosystem models particularly in a future scenario where nutrient
321 deplete gyre regions are set to expand (11).

Materials and Methods:

Bacteria and ciliate strains and cultivation conditions: Bacteria and ciliate strains used in this study is shown in Supplementary Table S2. *Phaeobacter* sp. MED193 was maintained in Marine Broth (MB) (Difco™ 2216; BD, Franklin Lakes, NJ, USA). A previously constructed *Phaeobacter* sp. MED193 Δ*plcP* mutant, unable to perform lipid remodelling, was also used (14). Bacteria were cultivated in Erlenmeyer flasks containing 40 mL modified artificial seawater (ASW) (58, 59), comprising sodium chloride 25 g/L, magnesium chloride hexahydrate 2 g/l, potassium chloride 0.5 g/l, calcium chloride dihydrate 0.5 g/l, magnesium sulfate 1.75 g/l, potassium dihydrogene phosphate 344.6 µM, HEPES 10 mM (pH 8.0), ammonium chloride 0.4078 g/l and sodium succinate 10 mM. The final pH of the medium was adjusted to 7.6. After autoclaving, the medium was supplemented with 1 mL trace metal solution (58, 59) and 1 mL vitamin solution (60). Cultures were incubated at 30°C with shaking at 180 rpm until stationary phase. To induce lipid remodelling, cells were harvested by centrifugation and washed three times before being re-suspended in ASW medium either replete (344.6 µM) or deplete (0 µM) in phosphate and incubated at 30°C with shaking at 180 rpm for 36 hr.

Axenic *Uronema marinum*, originally isolated from coastal seawater from Qingdao, China (61), was grown in 25 cm^2 tissue culture flasks (Corning® Falcon™, Corning, NY, USA) containing 20 mL Rich's medium at 22.5°C. Rich's medium was modified from the artificial seawater for protozoa (CCAP) and additionally contained 15 g/L protease/peptone (Oxoid, Basingstoke, UK), 5 g/L yeast extract (Sigma-Aldrich, Saint Louis, MO, USA), 10 g/L Complan (Heinz, Pittsburgh, PA, USA), 200 mL/L Leibovotz's L-15 (Fisher, Watham, MA, USA) and 0.1 M glucose. Medium was adjusted to pH 7.6-7.8 with 2 M sodium hydroxide and autoclaved at 120°C for 20 min. The axenic nature of the ciliate was routinely monitored by DAPI staining.

Enumeration of *Uronema*: *Uronema* growth kinetics were carried out over a time course of 72h in 96-well microplates. After rapid fixation with 10% Lugol iodine, the concentration of the ciliate suspension was assessed using a Malassez cell counting chamber.

Lipid analysis: Bacterial lipids were extracted using a modified Folch extraction protocol as described previously (62, 63). Briefly 1mL culture (OD_{600nm}=0.5) was collected by centrifugation. Total lipids were then extracted using methanol-chloroform, dried under nitrogen gas and the pellet re-suspended in 1 mL solvent (95%(v/v) liquid chromatography-mass spectrometry (LC-MS) grade acetonitrile, 5 % 10 mM ammonium acetate pH 9.2 in water). Bacterial lipids were analysed by LC-MS using a Dionex 3400RS HPLC with a HILIC BEH amide XP column (2.5 μm, 3.0x150 mm, Waters) coupled with an amaZon SL ion trap MS (Bruker) via electrospray ionisation (ESI) in both positive (+ve) and negative (-ve) ionisation mode. Data analysis was carried out using Bruker Compass software package.

Concanavalin A staining of bacteria: After growth in P-replete or P-deplete ASW medium, bacterial cultures were collected by centrifugation and the OD_{600nm} adjusted to 0.1. Then, 1 mL of the different suspensions were inoculated in triplicate into 24 well plates containing a coverslip previously coated with poly-D-Lysine (MW 70,000-150,000, Sigma-Aldrich, Saint Louis, MO, USA). Afterwards, the samples were directly fixed by adding formaldehyde at 4% (v/v) for 20 min and a low-speed centrifugation (15 min at 900 g) was used to initiate and increase cell adhesion to the coverslips. Finally, cells were stained with DAPI (5 μg/mL) and Concanavalin A (ConA) tetramethylrhodamine conjugate (Thermo Fisher Scientific, Waltham, MA, United States) (20 μg/mL) (39) and mounted with a drop of Mowiol antifade before observation using a confocal laser scanning microscope (CLSM, Zeiss LSM 880, Göttingen, Germany). Bacterial biovolumes and the biovolume of ConA-stained glycoconjugates in confocal laser scanning microscopy (CLSM) images were determined using 5 images for each of the three replicates using COMSTAT software developed in MATLAB R2015a (MathWorks, Natick, MA, United States) as described previously (64). Bacterial cell length was calculated from measurements made using at least 300 cells for each of the three replicates using MicrobeJ software (65) developed in Fiji 2.1.0/1.53c.

Prey labelling using fluorescent proteins: To visualize prey within protozoa, plasmids pBBR-KanR-p(aphII)-sfGFP and pBBR-KanR-p(aphII)-mcherry were generated that constitutively express a green fluorescent protein (GFP) or mcherry, respectively. The constitutive promoter of the aminoglycoside phosphotransferase II (*aph*II) was amplified by PCR as described previously (66) and Gibson assembly used to drive expression of each fluorescent protein in the broad-host-range cloning vector pBBR1 MCS-2 (67) forming pBBR-GentR-p(aphII)-sfGFP and pBBR-KanR-p(aphII)-mcherry. These plasmids were transformed into *Escherichia coli* S17.1 λ-pir via electroporation and mobilized into WT *Phaeobacter* sp. MED193 and the *plcP* mutant via conjugation (**Supp. Table S2**), using ½ YTSS as the medium (DSMZ). Transconjugants were selected using gentamicin (10 μg/mL) or kanamycin (50 μg/mL) on sea salts minimal medium containing artificial sea salts 30 g/L, sodium phosphate 1 mM, HEPES 10 mM (pH 8.0), $FeCl_2$ 5 μM, glucose (3 mM), succinate (5 mM), a mixture of vitamins (68) and glycine betaine (2mM) as the sole nitrogen source as previously described (69).

Interaction of the ciliate with a single prey: To initiate physical interaction between the predator and prey and to avoid growth of the prey during interactions, bacteria and protozoa were transferred to ASW medium deplete in either a carbon source (succinate) or phosphate. Protozoan suspensions were inoculated into 96 well plates at $1X10^4$ cells/mL. The prey (WT *Phaeobacter* sp. MED193 or the *plcP* mutant) were inoculated at a multiplicity of infection (MOI) of 10, 100 or 500 (equivalent to 10, 100 or 500 prey per protist cell, respectively). After 3h, 10h, 24h and 48h of contact time at 22.5°C, ciliates were treated with Triton™ X-100 (0.05%) for 30 min on ice and mechanically lysed by mixing using a syringe and 25g needle (BD, Franklin Lakes, NJ, USA) as described previously (39). Bacterial prey numbers were quantified by serial dilution on marine broth agar plates.

Interaction of the ciliate with two prey types: To initiate interaction of the ciliate with a two-prey mix, prey and ciliate were transferred into ASW medium containing 2.5 mM succinate and 86 μM phosphate (25% of the normal concentration) in order to limit prey growth. The ciliate was inoculated

400 at $1x10^4$ cells/mL whereas bacteria were inoculated at an MOI of 50 for each prey type (i.e., a MOI of
401 100 for total bacteria) using 24 well plates. After 5 min, 3h, 10h or 24h of contact time at 22.5°C
402 samples were directly fixed by adding formaldehyde at 4% (v/v) for 30 min, then a coverslip previously
403 coated with poly-L-Lysine was deposited in each well. Low speed centrifugation (15 min at 900 g) was
404 used to initiate and increase cell adhesion to the coverslips. Finally, *U. marinum* cells were stained
405 with DAPI and mounted with a drop of Mowiol antifade as described above before observation using
406 CLSM.
407
408 **Visualisation of prey inside *U. marinum* using CLSM:** Once the prey-ciliate interaction was initiated,
409 subsamples of the ciliates after 5 min, 3h, 10h and 24h of contact time were stained with DAPI (5
410 μg/mL) to visualise the ciliate nucleus. After 3h of contact time *Uronema* cells were treated with
411 LysoTracker™ Red DND-99 (Fisher, Watham, MA, USA) (70 nM final concentration) for 30 min to stain
412 lysosomal acidic compartments to observe the digestion process. To assess the involvement of
413 mannose receptors in prey capture by *Uronema,* protists were pre-incubated for 30 min with 20 μM
414 BSA-mannose to mask these receptors according to Wootton et al. (2007) prior to prey interaction
415 (38). Afterwards, samples were directly fixed by adding formaldehyde 4% (v/v) for 30 min.
416 Subsequently, a coverslip previously coated with poly-D-Lysine was deposited in each well. Low speed
417 centrifugation (15 min at 900 g) was used to initiate and increase cell adhesion to the coverslips.
418 Finally, cells were mounted with a drop of Mowiol antifade before observation using CLSM.
419
420 **Analysis of *plcP* transcripts in the *Tara* Oceans database:** Tara Oceans metagenomes (OM-RGCv2+G)
421 and metatranscriptomes (OM-RGCv2+T) were queried using *Phaeobacter* sp. MED193 PlcP via the
422 Ocean Gene Atlas web portal (18). *plcP* abundance in both metagenomes and metatranscriptomes
423 was obtained using hmmsearch with an expect threshold of $1e^{-40}$ normalised to the median abundance
424 of ten single copy marker genes (70, 71)**.**
425

Statistics: For each experiment, at least three biological replicates were performed and ≥100 protist cells per replicate were counted. To test for statistically significant differences (p<0.05) between two conditions a T-test was performed and a one-way analysis of variance including the Bonferroni post-test were performed to compare more than two conditions. The Wilcoxon-Mann-Whitney test was used to test for statistically significant differences (p<0.05) between the distribution of data obtained between two conditions. These tests were performed using SPSS 26.0 (IBM, Armonk, NY, USA).

Acknowledgements

This project received funding from the European Research Council (ERC) under the European Union's Horizon 2020 research and innovation program (grant agreement no. 726116). We thank Prof Jarone Pinhassi (Linnaeus University, Sweden) for providing wild-type *Phaeobacter* sp. MED193. We thank the Imaging Suite at the School of Life Sciences, University of Warwick for the use of Zeiss LSM 880 confocal microscope and NERC Strategic Environmental Capital Call for funding the amaZon SL ion trap MS for lipidomics.

Conflict of interest

The authors have no conflict of interest to declare.

Figure legends

Figure 1. Global prevalence and expression of the *plcP* gene and geographic distribution of *Uronema* sp. in marine systems. The distribution of the *plcP* gene in the global ocean (surface waters only) using the Tara Oceans dataset. The area of each bubble represents normalized *plcP* gene (**A**) or transcripts (**B**) abundance as the percentage of the median of ten prokaryotic single copy marker genes/transcripts at each sampling site. The Ocean Gene Atlas (OGA) database was searched using *plcP* of *Phaeobacter* sp. MED193 with an e-value cut-off of e^{-40}. (AO = Arctic Ocean, IO = Indian Ocean, MS = Mediterranean Sea, NAO = North Atlantic Ocean, NPO = North Pacific Ocean, RS = Red Sea, SAO = South Atlantic Ocean, SO = Southern Ocean, SPO = South Pacific Ocean). (**C**) Geographic distribution based on culture isolation and molecular detection of *Uronema marinum* strains around the world from various representative studies (**Supp. Table S1**).

Figure 2. Lipid remodelling facilitates prey escape from ingestion by the marine ciliate *Uronema marinum*. Confocal laser scanning microscopy images showing green fluorescent protein (GFP) labelled wild-type (WT) prey (**A**) or the Δ*plcP* mutant (**B**) inside the predator. WT and mutant prey cells were grown under either P-replete or P-deplete conditions. Formation of the surrogate lipid diacylglyceryl trimethylhomoserine (DGTS) is a hallmark event for lipid remodelling which was observed only in the WT prey cultivated in P-deplete conditions (**C**). Both ingestion rate (**D**) and the percentage of prey inside the protist (**E**) revealed that lipid remodelled prey was less likely ingested by the ciliate. These experiments were carried out in three biological replicates and at least 100 ciliates were counted for each replicate. (**F**) Measurement of the cell length of WT and Δ*plcP* mutant cells. The measurements were carried out using MicrobeJ software with at least 300 cells for each of the three replicates. (**G, H**) Confocal laser scanning microscopy images (**H**) and biovolume quantification (**G**) showing detection of mannose-containing glycoconjugates by tetramethylrhodamine (TRITC, red)-labelled Concanavalin A lectin (ConA-TRITC). The ratio was expressed as the biovolume of ConA-stained glycoconjugates to the bacterial biovolume (DAPI, blue). Values are the mean of three

replicates; error bars represent standard deviations and asterisks indicate significant difference (**p < 0.01 and ***p < 0.001).

Figure 3. The marine ciliate *Uronema marinum* selectively ingests lipid unmodelled prey (**A**) Percentage of phagosomes containing WT prey grown under P-replete or P-deplete conditions (**left**), WT or Δ*plcP* mutant prey grown under P-replete conditions (**middle**) or WT and Δ*plcP* mutant prey grown under P-deplete conditions (**right**). Results were obtained from three independent biological replicates counting food vacuoles from n=100 ciliates. Values are the mean of three replicates; error bars represent standard deviations and asterisks indicate significant difference (*p < 0.05 and **p <0.01). (**B**) Confocal laser scanning microscopy images of prey inside the predator. Upper panel, WT grown under P-replete conditions (labelled with GFP) and WT grown under P-deplete conditions (labelled with mCherry); Middle panel, WT (labelled with mCherry) and the Δ*plcP* mutant (labelled with GFP) grown under P-replete conditions; Lower panel, WT (labelled with mCherry) and the Δ*plcP* mutant (labelled with GFP) grown under P-deplete conditions.

Figure 4. Lipid remodelled *Phaeobacter* sp. MED193 prey promotes better growth of *Uronema*. The abundance of *U. marinum* (**A and C**) and *Phaeobacter* sp. MED193 WT (**B**) and Δ*plcP* mutant (**D**) during interactions in P-replete (green) or P-deplete medium (blue) at a MOI 10 (dotted lines), MOI 100 (dashed lines) and MOI 500 (solid lines). *Uronema* cells were counted using a Malassez counting chamber over 72h interaction period, and *Phaeobacter* WT and Δ*plcP* mutant cells were counted over a 48h period of interaction with *Uronema*. Measurements were made using three biological replicates each with three technical replicates and error bars represent standard deviations.

Figure 5. A lipid remodelled prey is more susceptible to ciliate digestion inside the phagolysosome. **(A)** Confocal laser scanning microscopy images showing green fluorescent protein (GFP) labelled wild-type prey (**top**) or Δ*plcP* mutant prey (**bottom**) and acidification of the phagolysosomes (Lysotracker,

Red) during predation by *Uronema*. (**B**) The percentage of acidified phagolysosomes containing WT prey or Δ*plcP* mutant prey inside the predator. Values are the mean of three replicates; error bars represent standard deviations and asterisks indicate significant difference (**$p < 0.01$). (**C**) The percentage of phagolysosomes containing WT prey that had been grown under P-replete or P-deplete conditions. (**D**) The percentage of phagolysosomes containing either WT or Δ*plcP* mutant prey grown in P-replete medium (**E**) The percentage of phagolysosomes containing WT or Δ*plcP* mutant prey grown in P-deplete medium. For C-E results were obtained from three independent biological replicates from which vacuoles from n=100 ciliates/replicate were counted. Values are the mean of three replicates; error bars represent standard deviations and asterisks indicate significant difference (*$p < 0.05$, **$p<0.01$ and ***$p < 0.001$).

Figure 6 Proposed trade-off mechanism due to lipid remodelling of *Phaeobacter* sp. MED 193 when interacting with the predator *Uronema marinum.* *Phaeobacter* sp. MED193 grown in a P-deplete environment induces lipid remodelling in order to reduce its P quota and release phosphate for use in other major cellular processes. A lipid remodelled cell has a reduced level of mannose-containing macromolecules, making prey capture by *Uronema marinum* problematic. However, conversely a lipid remodelled prey is unable to prevent phagolysosomal acidification making it more susceptible to digestion by the ciliate which in turn facilitates better ciliate growth.

References:

1. K. R. Arrigo, Marine microorganisms and global nutrient cycles. *Nature* **437**, 349-355 (2005).
2. E. L. Madsen, Microorganisms and their roles in fundamental biogeochemical cycles. *Curr Opin Biotechnol* **22**, 456-464 (2011).
3. S. L. Strom, Microbial ecology of ocean biogeochemistry: a community perspective. *Science* **320**, 1043-1045 (2008).
4. C. M. Moore *et al.*, Processes and patterns of oceanic nutrient limitation. *Nature Geosci* **6**, 701-710 (2013).
5. H. Garcia *et al.*, World Ocean Atlas 2013, Volume 4: Dissolved inorganic nutrients (Phosphate, Nitrate, Silicate), NOAA Atlas NESDIS, vol. 76, edited by S. Levitus, 25 pp. *US Gov. Print. Off., Washington, DC* (2014).
6. O. A. Sosa, D. J. Repeta, E. F. DeLong, M. D. Ashkezari, D. M. Karl, Phosphate-limited ocean regions select for bacterial populations enriched in the carbon-phosphorus lyase pathway for phosphonate degradation. *Environ Microbiol* **21**, 2402-2414 (2019).
7. M. V. Zubkov *et al.*, Microbial control of phosphate in the nutrient-depleted North Atlantic subtropical gyre. *Environ Microbiol* **9**, 2079-2089 (2007).
8. S. T. Dyhrman, J. W. Ammerman, B. A. S. van Mooy, Microbes and the marine phosphorus cycle. *Oceanography* **20** (2007).
9. T. F. Thingstad *et al.*, Nature of phosphorus limitation in the ultraoligotrophic eastern Mediterranean. *Science* **309**, 1068-1071 (2005).
10. T. F. Thingstad, U. L. Zweifel, F. Rassoulzadegan, P limitation of heterotrophic bacteria and phytoplankton in the northwest Mediterranean. *Limnol Oceanogr* **43**, 88-94 (1998).
11. J. J. Polovina, E. A. Howell, M. Abecassis, Ocean's least productive waters are expanding. *Geophys Res Lett* **35** (2008).
12. B. A. van Mooy *et al.*, Phytoplankton in the ocean use non-phosphorus lipids in response to phosphorus scarcity. *Nature* **458**, 69-72 (2009).
13. P. Carini *et al.*, SAR11 lipid renovation in response to phosphate starvation. *Proc Natl Acad Sci U S A* **112**, 7767-7772 (2015).
14. M. Sebastian *et al.*, Lipid remodelling is a widespread strategy in marine heterotrophic bacteria upon phosphorus deficiency. *ISME J* **10**, 968-978 (2016).
15. E. Silvano *et al.*, Lipidomic analysis of *Roseobacters* of the pelagic RCA cluster and their response to phosphorus limitation. *Front Microbiol* **11**, 552135 (2020).
16. H. Luo, M. A. Moran, Evolutionary ecology of the marine *Roseobacter* clade. *Microbiol Mol Biol Rev* **78**, 573-587 (2014).
17. M. A. Moran *et al.*, Ecological genomics of marine *Roseobacters*. *Appl Environ Microbiol* **73**, 4559-4569 (2007).
18. E. Villar *et al.*, The ocean gene atlas: exploring the biogeography of plankton genes online. *Nucleic Acids Res* **46**, W289-W295 (2018).
19. S. J. Giovannoni, J. Cameron Thrash, B. Temperton, Implications of streamlining theory for microbial ecology. *ISME J* **8**, 1553-1565 (2014).
20. D. O. Hessen, P. D. Jeyasingh, M. Neiman, L. J. Weider, Genome streamlining and the elemental costs of growth. *Trends Ecol Evol* **25**, 75-80 (2010).
21. J. Pernthaler, Predation on prokaryotes in the water column and its ecological implications. *Nat Rev Microbiol* **3**, 537-546 (2005).
22. M. Breitbart, C. Bonnain, K. Malki, N. A. Sawaya, Phage puppet masters of the marine microbial realm. *Nat Microbiol* **3**, 754-766 (2018).
23. L. Riemann, M. Middelboe, Viral lysis of marine bacterioplankton: Implications for organic matter cycling and bacterial clonal composition. *Ophelia* **56**, 57-68 (2002).
24. H. Takasu, T. Kunihiro, S.-i. Nakano, Protistan grazing and viral lysis losses of bacterial carbon production in a large mesotrophic lake (Lake Biwa). *Limnology* **15**, 257-270 (2014).

25. C. Matz, K. Jurgens, Interaction of nutrient limitation and protozoan grazing determines the phenotypic structure of a bacterial community. *Microb Ecol* **45**, 384-398 (2003).
26. C. L. Meunier, K. Schulz, M. Boersma, A. M. Malzahn, Impact of swimming behaviour and nutrient limitation on predator–prey interactions in pelagic microbial food webs. *J Exp Mar Biol Ecol* **446**, 29-35 (2013).
27. C. de Vargas *et al.*, Ocean plankton. Eukaryotic plankton diversity in the sunlit ocean. *Science* **348**, 1261605 (2015).
28. D. A. Caron, P. D. Countway, A. C. Jones, D. Y. Kim, A. Schnetzer, Marine protistan diversity. *Ann Rev Mar Sci* **4**, 467-493 (2012).
29. D. A. Caron, A. Z. Worden, P. D. Countway, E. Demir, K. B. Heidelberg, Protists are microbes too: a perspective. *ISME J* **3**, 4-12 (2009).
30. A. Gimmler, R. Korn, C. de Vargas, S. Audic, T. Stoeck, The Tara Oceans voyage reveals global diversity and distribution patterns of marine planktonic ciliates. *Sci Rep* **6**, 33555 (2016).
31. D. M. Needham *et al.*, Dynamics and interactions of highly resolved marine plankton via automated high-frequency sampling. *ISME J* **12**, 2417-2432 (2018).
32. T. M. Tsagaraki *et al.*, Bacterial community composition responds to changes in copepod abundance and alters ecosystem function in an Arctic mesocosm study. *ISME J* **12**, 2694-2705 (2018).
33. S. Muthusamy, F. Baltar, J. M. Gonzalez, J. Pinhassi, Dynamics of metabolic activities and gene expression in the *Roseobacter* clade bacterium *Phaeobacter* sp. strain MED193 during growth with thiosulfate. *Appl Environ Microbiol* **80**, 6933-6942 (2014).
34. I. Dykova, T. Tyml, M. Kostka, H. Peckova, Strains of *Uronema marinum* (Scuticociliatia) co-isolated with amoebae of the genus *Neoparamoeba*. *Dis Aquat Organ* **89**, 71-77 (2010).
35. B. Pérez-Uz, Growth rate variability in geographically diverse clones of *Uronema* (Ciliophora: Scuticociliatida). *FEMS Microbiol Ecol* **16**, 193-203 (1995).
36. A. Jousset, Ecological and evolutive implications of bacterial defences against predators. *Environ Microbiol* **14**, 1830-1843 (2012).
37. N. Yutin, M. Y. Wolf, Y. I. Wolf, E. V. Koonin, The origins of phagocytosis and eukaryogenesis. *Biol Direct* **4**, 9 (2009).
38. E. C. Wootton *et al.*, Biochemical prey recognition by planktonic protozoa. *Environ Microbiol* **9**, 216-222 (2007).
39. R. Guillonneau, C. Baraquet, M. Molmeret, Marine bacteria display different escape mechanisms when facing their protozoan predators. *Microorganisms* **8** (2020).
40. M. W. Hahn, H. Lünsdorf, L. Janke, Exopolymer production and microcolony formation by planktonic freshwater bacteria: defence against protistan grazing. *Aquat Microb Ecol* **35**, 297-308 (2004).
41. W. Sunda, D. Hardison, Evolutionary tradeoffs among nutrient acquisition, cell size, and grazing defense in marine phytoplankton promote ecosystem stability. *Mar Ecol Prog Ser* **401**, 63-76 (2010).
42. V.-P. Friman, M. Ghoul, S. Molin, H. K. Johansen, A. Buckling, *Pseudomonas aeruginosa* adaptation to lungs of cystic fibrosis patients leads to lowered resistance to phage and protist enemies. *PLoS One* **8**, e75380 (2013).
43. H. Wildschutte, D. M. Wolfe, A. Tamewitz, J. G. Lawrence, Protozoan predation, diversifying selection, and the evolution of antigenic diversity in *Salmonella*. *Proc Natl Acad Sci U S A* **101**, 10644-10649 (2004).
44. E. C. Roberts, C. Legrand, M. Steinke, E. C. Wootton, Mechanisms underlying chemical interactions between predatory planktonic protists and their prey. *J Plankton Res* **33**, 833-841 (2011).
45. C. M. Martel, Nitrogen-deficient microalgae are rich in cell-surface mannose: potential implications for prey biorecognition by phagotrophic protozoa. *Braz J Microbiol* **40**, 86-89 (2009).

46. C. M. Martel, Conceptual bases for prey biorecognition and feeding selectivity in the microplanktonic marine phagotroph *Oxyrrhis marina*. *Microb Ecol* **57**, 589-597 (2009).
47. E. van Donk, D. O. Hessen, Grazing resistance in nutrient-stressed phytoplankton. *Oecologia* **93**, 508-511 (1993).
48. A. Dadon-Pilosof *et al.*, Surface properties of SAR11 bacteria facilitate grazing avoidance. *Nat Microbiol* **2**, 1608-1615 (2017).
49. S. P. Shannon, T. H. Chrzanowski, J. P. Grover, Prey food quality affects flagellate ingestion rates. *Microb Ecol* **53**, 66-73 (2007).
50. G. Weiss, U. E. Schaible, Macrophage defense mechanisms against intracellular bacteria. *Immunol Rev* **264**, 182-203 (2015).
51. J. Petersen, O. Frank, M. Göker, S. Pradella, Extrachromosomal, extraordinary and essential—the plasmids of the *Roseobacter* clade. *Appl Microbiol and Biotechnol* **97**, 2805-2815 (2013).
52. M. R. Seyedsayamdost, R. J. Case, R. Kolter, J. Clardy, The Jekyll-and-Hyde chemistry of *Phaeobacter gallaeciensis*. *Nat Chem* **3**, 331-335 (2011).
53. H. Wang, J. Tomasch, M. Jarek, I. Wagner-Dobler, A dual-species co-cultivation system to study the interactions between *Roseobacters* and dinoflagellates. *Front Microbiol* **5**, 311 (2014).
54. M. Z. Wilson, R. Wang, Z. Gitai, M. R. Seyedsayamdost, Mode of action and resistance studies unveil new roles for tropodithietic acid as an anticancer agent and the γ-glutamyl cycle as a proton sink. *Proc Natl Acad Sci U S A* **113**, 1630-1635 (2016).
55. B. A. Van Mooy, G. Rocap, H. F. Fredricks, C. T. Evans, A. H. Devol, Sulfolipids dramatically decrease phosphorus demand by picocyanobacteria in oligotrophic marine environments. *Proc Natl Acad Sci U S A* **103**, 8607-8612 (2006).
56. E. N. Reistetter *et al.*, Effects of phosphorus starvation versus limitation on the marine cyanobacterium *Prochlorococcus* MED4 II: gene expression. *Environ Microbiol* **15**, 2129-2143 (2013).
57. J. Pinhassi *et al.*, Seasonal changes in bacterioplankton nutrient limitation and their effects on bacterial community composition in the NW Mediterranean Sea. *Aquat Microb Ecol* **44**, 241-252 (2006).
58. W. H. Wilson, N. G. Carr, N. H. Mann, The effect of phosphate status on the kinetics of cyanophage infection in the oceanic cyanobacterium *Synechococcus* sp. wh7803 1. *J Phycol* **32**, 506-516 (1996).
59. M. Wyman, R. Gregory, N. Carr, Novel role for phycoerythrin in a marine cyanobacterium, *Synechococcus* strain DC2. *Science* **230**, 818-820 (1985).
60. T. Kanagawa, M. Dazai, S. Fukuoka, Degradation of O, O-dimethyl phosphorodithioate by *Thiobacillus thioparus* TK-1 and *Pseudomonas* AK-2. *Agric Biol Chem* **46**, 2571-2578 (1982).
61. Z. J. Teng *et al.*, Acrylate protects a marine bacterium from grazing by a ciliate predator. *Nat Microbiol* **6**, 1351-1356 (2021).
62. J. Folch, M. Lees, G. H. Sloane Stanley, A simple method for the isolation and purification of total lipides from animal tissues. *J Biol Chem* **226**, 497-509 (1957).
63. A. F. Smith *et al.*, Elucidation of glutamine lipid biosynthesis in marine bacteria reveals its importance under phosphorus deplete growth in *Rhodobacteraceae*. *ISME J* **13**, 39-49 (2019).
64. A. Heydorn *et al.*, Quantification of biofilm structures by the novel computer program COMSTAT. *Microbiology* **146**, 2395-2407 (2000).
65. A. Ducret, E. M. Quardokus, Y. V. Brun, MicrobeJ, a tool for high throughput bacterial cell detection and quantitative analysis. *Nat Microbiol* **1**, 16077 (2016).
66. T. Piekarski *et al.*, Genetic tools for the investigation of *Roseobacter* clade bacteria. *BMC Microbiol* **9**, 265 (2009).
67. M. E. Kovach *et al.*, Four new derivatives of the broad-host-range cloning vector pBBR1MCS, carrying different antibiotic-resistance cassettes. *Gene* **166**, 175-176 (1995).

68. Y. Chen, N. A. Patel, A. Crombie, J. H. Scrivens, J. C. Murrell, Bacterial flavin-containing monooxygenase is trimethylamine monooxygenase. *Proc Natl Acad Sci U S A* **108**, 17791-17796 (2011).
69. I. Lidbury, J. C. Murrell, Y. Chen, Trimethylamine N-oxide metabolism by abundant marine heterotrophic bacteria. *Proc Natl Acad Sci U S A* **111**, 2710-2715 (2014).
70. A. Milanese *et al.*, Microbial abundance, activity and population genomic profiling with mOTUs2. *Nat Commun* **10**, 1014 (2019).
71. A. R. J. Murphy *et al.*, Transporter characterisation reveals aminoethylphosphonate mineralisation as a key step in the marine phosphorus redox cycle. *Nat Commun* **12**, 4554 (2021).

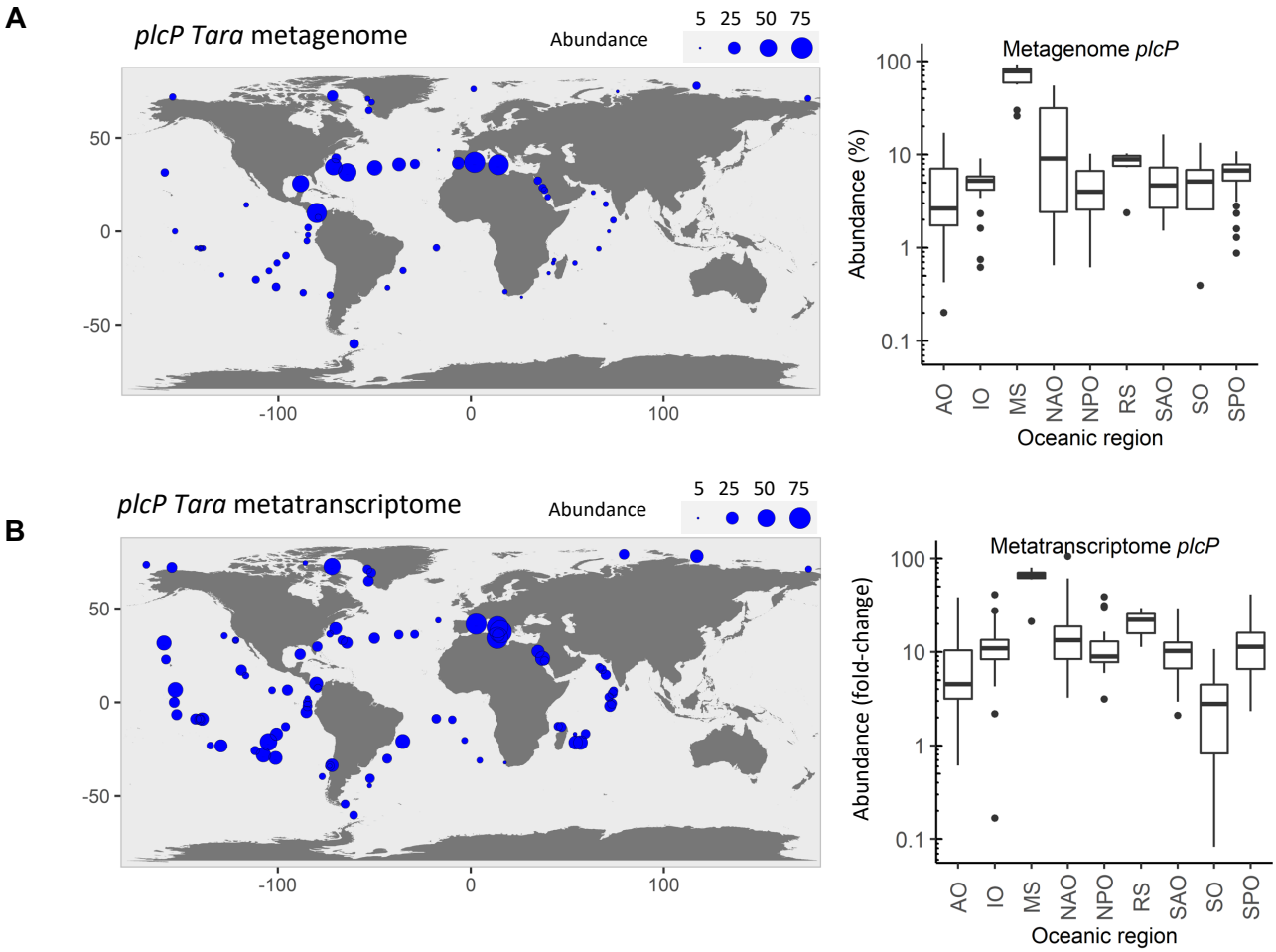
A
plcP Tara metagenome
Abundance
5 25 50 75
50
0
-50
-100
0
100
Metagenome plcP
Abundance (%)
100
10
1
0.1
AO
IO
MS
NAO
NPO
RS
SAO
SO
SPO
Oceanic region
B
plcP Tara metatranscriptome
Abundance
5 25 50 75
50
0
-50
-100
0
100
Metatranscriptome plcP
Abundance (fold-change)
100
10
1
0.1
AO
IO
MS
NAO
NPO
RS
SAO
SO
SPO
Oceanic region


C
Anderson et al., 2009 (isolation)
Coppellotti, 1994 (isolation)
Du et al., 2019 (isolation), Zheng et al., 2015 (isolation)
Dykova et al., 2010 (isolation and sequence)
First and Hollibaugh, 2009 (isolation)
Glud and Fenchel, 1999 (isolation)
Hannah and Lilly, 1974 (isolation)
Harikrishnan et al, 2011 (sequence), Song et al., 2009 (isolation)
Kalavati et al., 1997 (isolation)
Kaneshiro et al., 1976 (isolation)
Kwon et al., 2003 (isolation), Wang et al., 2013 (isolation)
Li et al., 2018 (sequence)
Nitsche and Arndt, 2015 (sequence)
Parker, 1976 (isolation)
Perez-Bustamante et al., 2021 (isolation)
Perez-Uz, 1995, (isolation)
Plunket and Hidu, 1978 (isolation)

Figure 1:

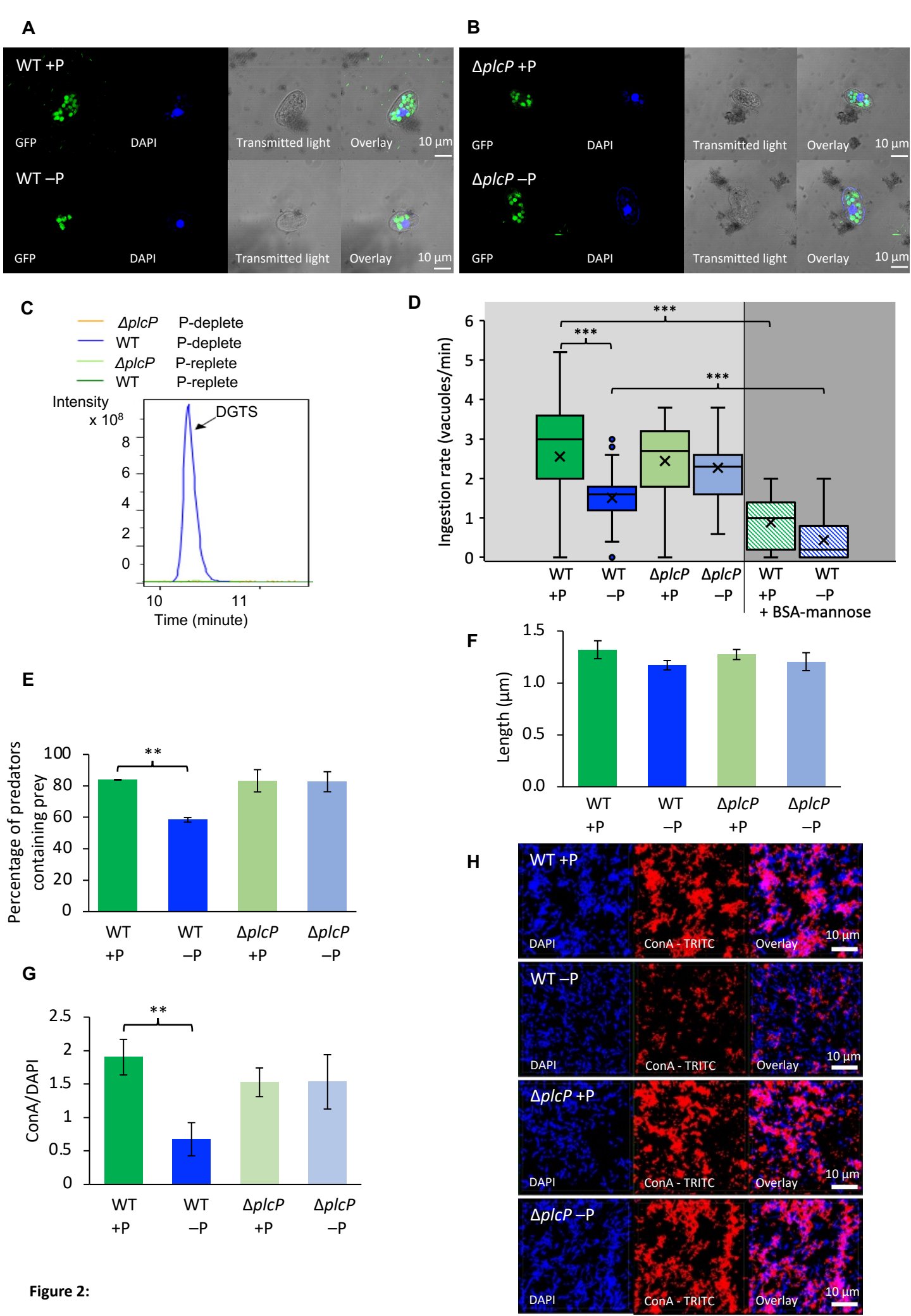
A
WT +P
GFP
DAPI
Transmitted light
Overlay
10 µm
WT –P
B
ΔplcP +P
ΔplcP –P
C
ΔplcP P-deplete
WT P-deplete
ΔplcP P-replete
WT P-replete
Intensity x 10^8
DGTS
Time (minute)
D
Ingestion rate (vacuoles/min)
***
WT +P
WT –P
ΔplcP +P
ΔplcP –P
+ BSA-mannose
E
Percentage of predators containing prey
**
F
Length (µm)
G
ConA/DAPI
H
ConA - TRITC

Figure 2:

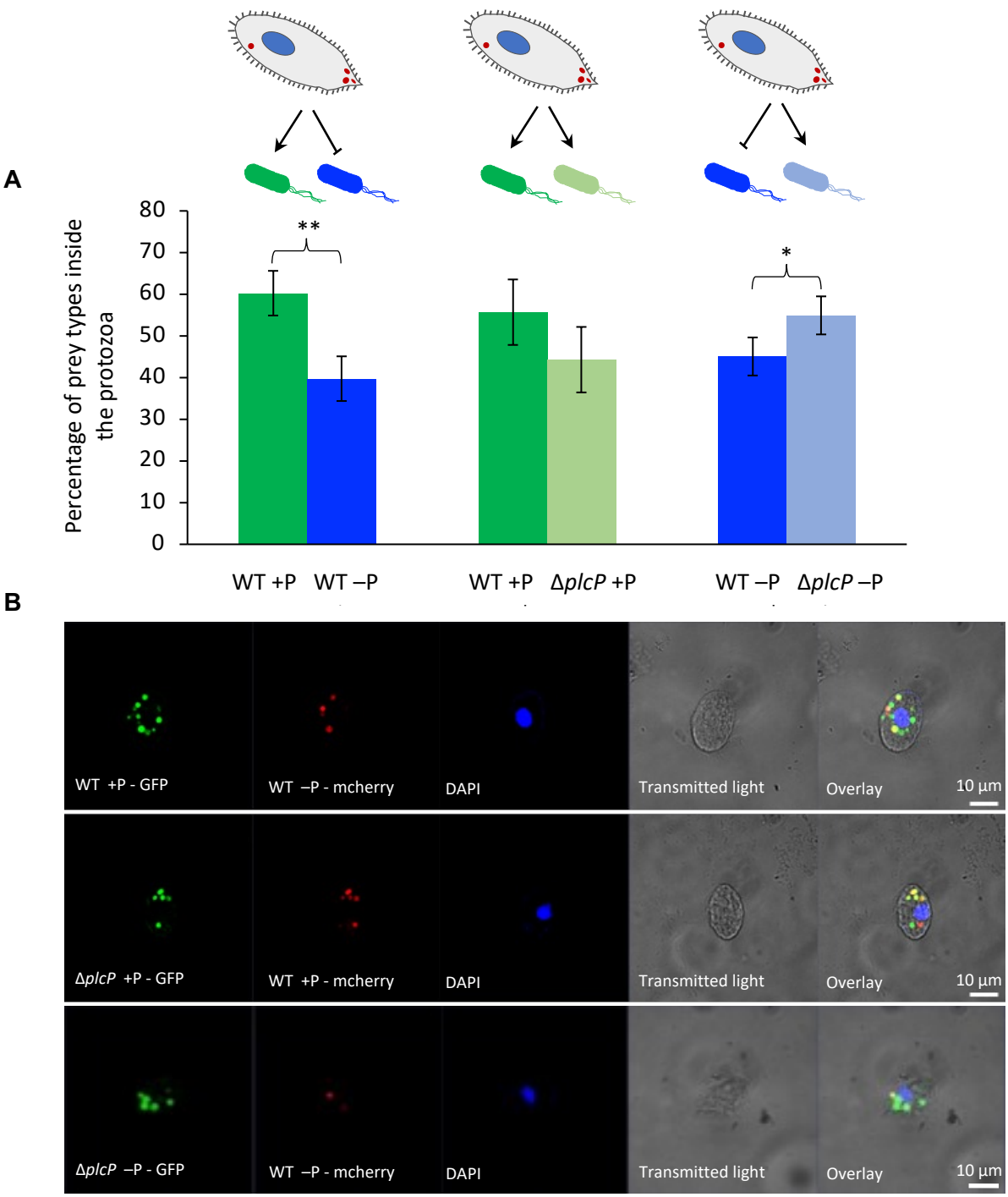
A
Percentage of prey types inside the protozoa
80
70
60
50
40
30
20
10
0
**
*
WT +P
WT –P
WT +P
ΔplcP +P
WT –P
ΔplcP –P
B
WT +P - GFP
WT –P - mcherry
DAPI
Transmitted light
Overlay
10 µm
ΔplcP +P - GFP
WT +P - mcherry
DAPI
Transmitted light
Overlay
10 µm
ΔplcP –P - GFP
WT –P - mcherry
DAPI
Transmitted light
Overlay
10 µm

Figure 3:

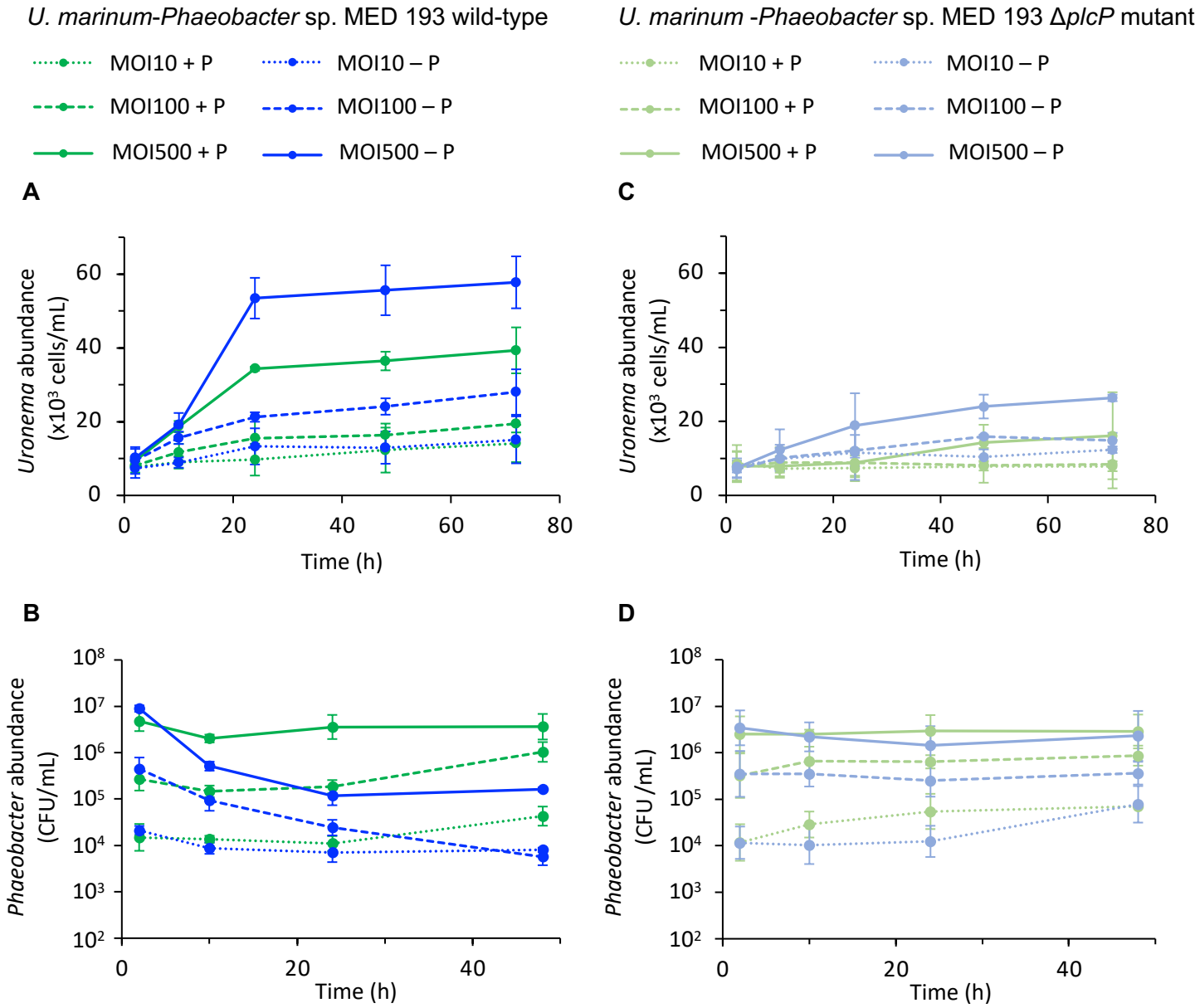
U. marinum-Phaeobacter sp. MED 193 wild-type
MOI10 + P
MOI10 – P
MOI100 + P
MOI100 – P
MOI500 + P
MOI500 – P
A
Uronema abundance (x10³ cells/mL)
Time (h)
U. marinum -Phaeobacter sp. MED 193 ΔplcP mutant
MOI10 + P
MOI10 – P
MOI100 + P
MOI100 – P
MOI500 + P
MOI500 – P
C
Uronema abundance (x10³ cells/mL)
Time (h)
B
Phaeobacter abundance (CFU/mL)
Time (h)
D
Phaeobacter abundance (CFU/mL)
Time (h)

Figure 4:

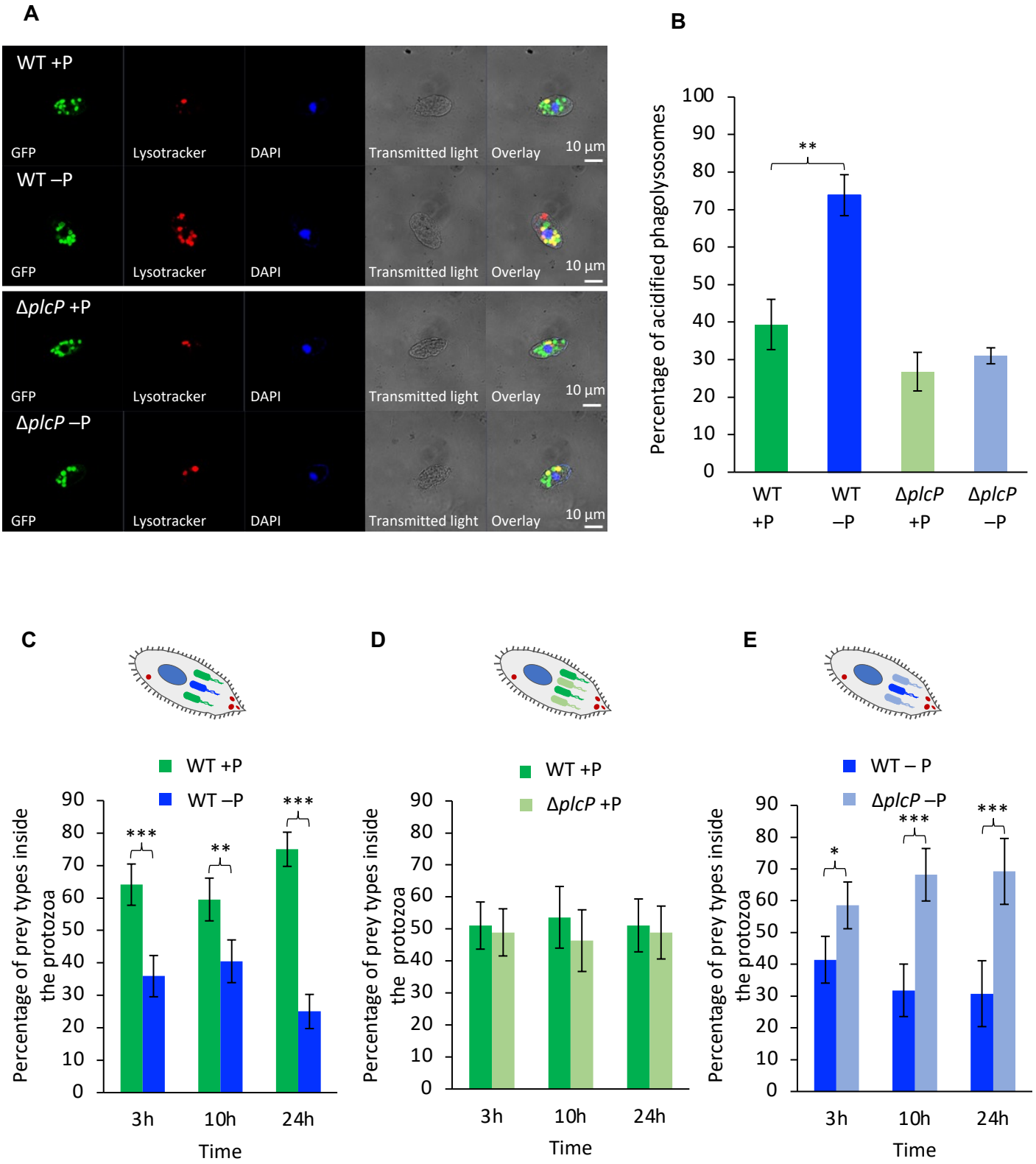
A
WT +P
GFP
Lysotracker
DAPI
Transmitted light
Overlay
10 µm
WT –P
ΔplcP +P
ΔplcP –P
B
Percentage of acidified phagolysosomes
**
WT +P
WT –P
ΔplcP +P
ΔplcP –P
C
WT +P
WT –P
Percentage of prey types inside the protozoa
***
**
***
3h
10h
24h
Time
D
WT +P
ΔplcP +P
E
WT – P
ΔplcP –P
*
***
***

Figure 5:

P replete (Prey do not perform lipid remodeling)

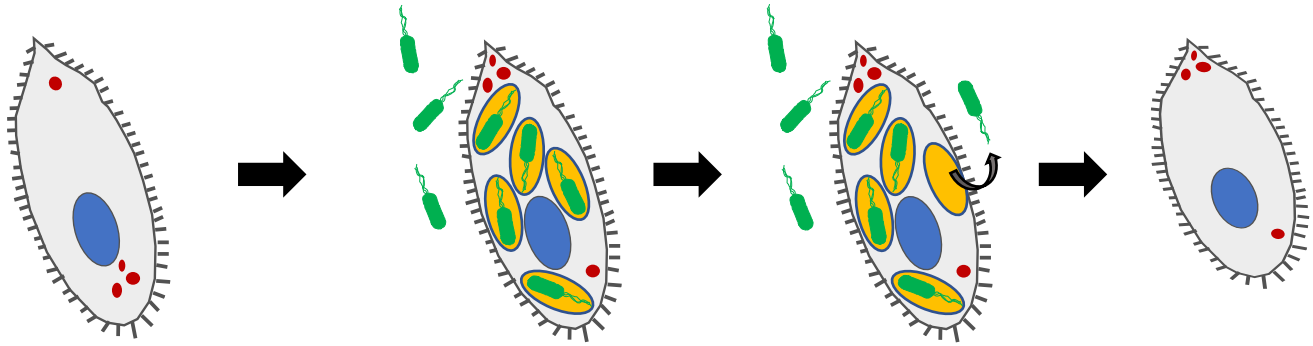

Prey encounter

Prey ingested

Prevention of phagosome acidification

No growth of predator

Legend:

Nucleus

Lysosome

Phagosome

Phagolysosome

Bacteria performing lipid remodeling

Bacteria secreting mannose-containing glycoconjugates

P deplete (prey perform lipid remodeling)

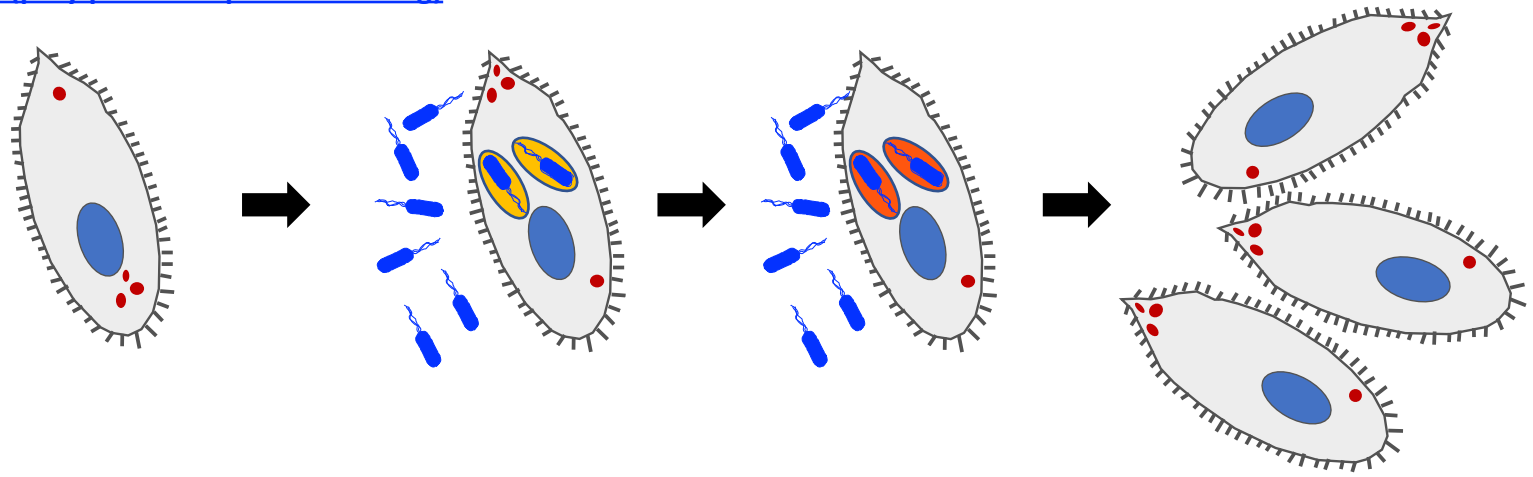

Prey encounter

Less prey ingested

Phagosome acidification

Growth of predator